

Spectroscopy of SiPM array detectors by digital spectroscopy method and implementing trapezoidal digital filter

Homa Berjisi^a, Ali Pazirandeh^{a,b,*}

^a Nuclear Engineering Department, Science and Research Branch, Islamic Azad University, Tehran, Iran

^b Physics Department, Tehran University, Tehran, Iran

H I G H L I G H T S

- In this article using 2×2 SiPM array coupled with CsI(Tl).
- Designing preamplifier circuit for each channel of SiPM, and also summed circuit to sum 4-channel of array.
- PWrite algorithm of trapezoidal digital filter.
- Using conventional Multichannel analyzer for summed channel and get spectrum.
- The algorithm for digital spectroscopy method has been compared with the analog method.

ABSTRACT

Digital spectroscopy with Silicon Photomultiplier (SiPM) array coupled on CsI(Tl) crystal, needs some consideration to achieve desirable energy resolution. an array of SiPMs must be used with large scintillation crystal, therewithal signal from whole SiPMs is not ideal. Also silicon pixels are arranged in arrays at regular intervals. The distances between the pixels and the interference of the cross-talk of adjacent pixels are undesirable factors for energy resolution when the light is received by the crystal and transmitted to the SiPM array. On the other hand, due to the advantages of the SiPM array, there is a need to improve the energy resolution in order to be able to be applied. In this paper, an attempt is made to obtain the desired energy resolution by using the digital spectroscopy method and digital filters and properly shaping the output pulse of the preamplifier by the trapezoidal filter method. In this case, it will be possible to use it in different applications such as spectroscopy by the detector.

KEY WORDS

SiPM
Energy Resolution
Preamplifier
Teraapezoidal Shaping
Spectroscopy

HISTORY

Received: 13 July 2022
Revised: 18 December 2022
Accepted: 22 December 2022
Published: Summer 2023

1 Introduction

SiPMs are a good alternative to Photomultiplier Tube (PMT) tubes due to their insensitivity to a magnetic field, small size, low bias voltage, and the lack of effect of time on their performance (Alispach et al., 2020; Henningsen et al., 2021; Sun and Maricic, 2016; Knoll, 2010; Czyz and Farsoni, 2017). SiPMs have many applications in various fields including light detection and its range Light Detection and Range (LiDAR) (Optical Imaging Systems) (Gnechi et al., 2019; Gnechi and Jackson, 2017; Jeong and Hammig, 2020; Shimazoe et al., 2020; Liang et al., 2020; Maira et al., 2020), medical imaging (Yang et al., 2019; Kitsmiller and OSullivan, 2019; Cates et al., 2017; Kim et al., 2021), and gamma radiation detection (Yang et al., 2019; Tétrault et al., 2015; Aldawood et al., 2017;

Lee et al., 2020; Cozzi et al., 2016; Boo et al., 2021; Xiong et al., 2019; Berti et al., 2020; Jiang et al., 2021). Thus, representing techniques for measuring and improving energy resolution plays an important role in spectroscopy. Two methods are used to read signals from SiPMs: the analog method and the digital method (Frach et al., 2009). The use of digital systems is a good option for accurate measurements. One of the advantages of these systems is the possibility of implementing optimal filters in order to achieve a better signal-to-noise ratio and correct the filter parameters compared to analog systems and improve the energy resolution. Other advantage of digital spectroscopy over analog spectroscopy are the removal of hardware and help to the reduction of the size of these systems. The good thing about doing this is that it flexes the system to make various changes to it, which allows

*Corresponding author: Pzrud193y@srbiau.ac.ir, paziran@mail.ut.ac.ir

<https://doi.org/10.22034/rpe.2022.351237.1095>

<https://dorl.net/dor/20.1001.1.26456397.2023.4.3.1.9>



Figure 1: SiPM with CsI(Tl) crystal and reflector.

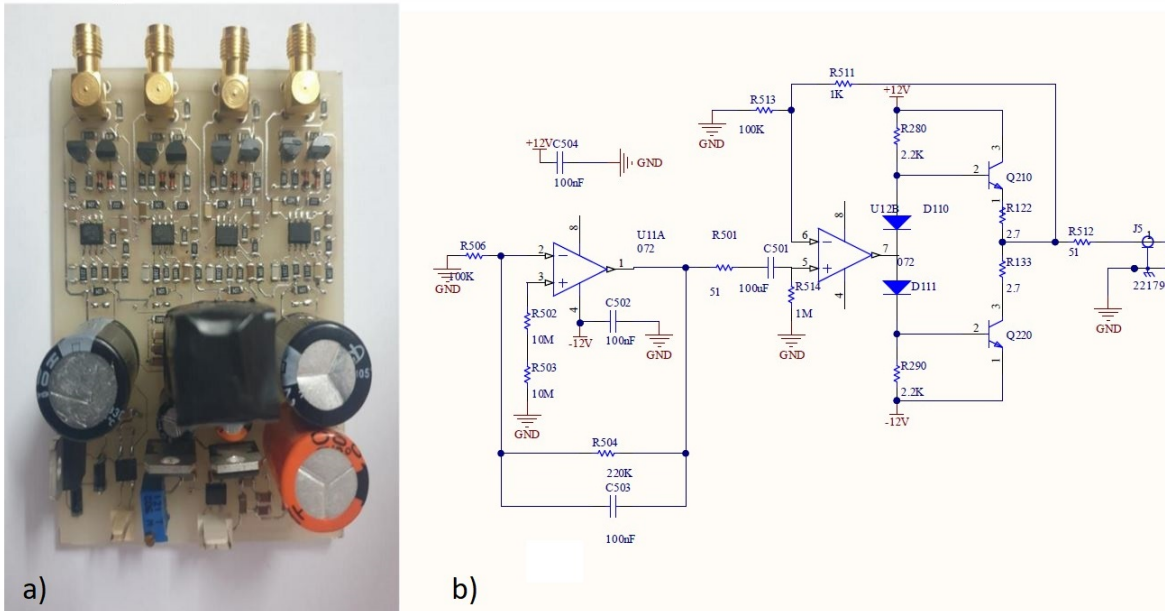


Figure 2: Four-channel amplifier board with detector power supply in dimensions 6 cm × 7 cm (b) schematic circuit of preamplifier.

for extensive changes without any hardware changes. On the other hand, there will be no noise from the electronic system such as thermal noise in these systems. As the pixels of SiPM array are not completely identical and also the quality of optical coupling between SiPM and crystal is not the same, the light collected by the crystal could be different in each pixel to another one. In digital spectroscopy, it is possible to sum different amounts of light collected and use some weighting factor to normalize the signal before summing them. Parameters such as pile up, dead time, and electronic noise in analog systems are destructive factors in spectroscopy. Trapezoidal filters are commonly used in digital spectroscopy processes in order to improve energy resolution by reducing noise. This process is done by averaging the peak time range (p) and calculating the difference between the two areas separated by a flattop and it is repeated for each point of the sample (CAEN, 2011). One of the major problems for the use of SiPM coupled with integrated CsI(Tl) crystal is a loss of energy resolution. According to the studies, two methods have been proposed: the active method and the passive one. In the passive method, the output of SiPM is given to adder energy resolution improved but the side of the pulse shape is not preserved. In the active method, the outputs of 4 SiPM from a 2×2 array are given to an ampli-

fier, and finally, with an output collector, they are fed to a multi-channel analyzer. This operation is repeated for the other arrays, respectively. It is well preserved, but the resolution is less favorable than the passive state (Lavelle et al., 2019). In our proposed method, a multichannel analyzer was applied to each element of the array and their spectrum by a simultaneous adder was added. The paper goal is to achieve the advantages of the previous method, namely the desired energy resolution and also maintaining the pulse shape. The following steps have been performed to prepare the test instrument including the detector and amplifier.

2 Material and Methods

In order to provide the required data for the spectroscopy of SiPM array detectors by digital spectroscopy method, an experimental setup was designed which was shown in Fig. 1.

In the experimental setup, a polished CsI (Tl) crystal together with Teflon tape as a reflector was coupled on the SiPM (60035, 2×2 array, Sensel Co.) surface with scintillation Silicon grease (BC-631, Saint Gobain Co.) (Fig. 1).

The 4-channel, fast and low noise preamplifier applied

to use with the array detector along with its power supply and schematic circuit of this Printed Circuit Board (PCB) is shown in can be seen in (Fig. 2). The bias voltage of each SiPM is 24 Volt.

The integrated CsI(Tl) and Array 2×2 of SiPM was coupled. SiPM/CsI(Tl) crystal dimensions of 14 mm \times 14 mm \times 15 mm (crystal dimensions are about one millimeter smaller than the margin of the arrays compared to the effective surface of the SiPM array). The other parts of the crystal are covered with the reflectors. According to the studies, the use of a guide between the crystal surface and the optical-silicon amplifier does not have the desired result (Huang et al., 2017). Therefore, an array of SiPM is used while using a large surface area of scintillators. The output is given to a four-channel digitizer system, in which the output of each silicon SiPM array pixel is connected to a channel of the digitizer, and each pixel is given separately to a pre-amplifier designed for this application in this study. On the other hand, the output of the pre-amplifiers can be connected to 4 multi-channel analyzers and the spectrum obtained from these analyzers can be added together.

In this research, a low noise charge-sensitive preamplifier and amplifier have been used (Fig. 2). The output of the CsI(Tl) detector is connected to the zero to third input of the digitizer. As can be seen in Fig. 3, the output of the CAEN model 1721 digitizer has been used. After making the necessary adjustments to its output digitizer, the digitized output has been received and a trapezoidal filter has been applied to the input. The written algorithm is given in this research.

3 Result of Measurements

3.1 Trapezoidal filter

Trapezoidal filter is one of the most widely used types of the digital filters for pulse processing relevant to the nuclear radiation detectors. Applying trapezoidal formation (trapezoidal filter) is one of the methods of extracting the information of the detector output signal. One of the advantages of pulse shaping in this way is reducing noise and improving energy resolution. There are different algorithms for applying this filter to the output pulse of the amplifier (Knoll, 2010) Digital filters such as finite impulse response (FIR) (Press et al., 2007) which is in impulse response of a limited time interval. In contrast there are filters (IIR) that can have internal feedback and have unlimited and continuous responses. In this research, the recursive shaping algorithm (Eq. (1)) has been used (Gnechi and Jackson, 2017). A part of the code, written for this recursive algorithm, is also visible along with the relation.

$$y(n) = \sum_{k=0}^N h(k) \cdot (n - k) \quad (1)$$

where $h(k)$ is the signal impulse response, the convolution of which is calculated in the recursive function.

Convolution determines the relationship between the input signal and the output signal. The results of applying the algorithm to the amplifying signal can be seen in

Fig. 5 and Fig. 6. As can be seen in Fig. 6, the trapezoidal algorithm worked correctly on successive pulses, while the flattop in Figs. 6-B and 6-C is without slope and completely smooth, but in Fig. 6-A, we see it as slope. In order to correct this condition and smooth the flattop for all input pulses, it is necessary to optimize the digital trapezoidal filter parameters. In the analog systems, it was applied as the hardware.



Figure 3: CAEN digital system including digitizer cards, TDC (Time to Digital convertor), Bridge trapezoidal pulse reset.

```
xnk = xnd = xndk = 0
for n in range(1+k+d, s):
    if n-k<0 : xnk = 0
    else: xnk = x[n-k]
    if n-d<0 : xnd = 0
    else: xnd = x[n-d]
    if n-d-k<0 : xndk = 0
    else: xndk = x[n-d-k]
    y[n] = y[n-1] + x[n] - xnk - xnd + xndk
```

Figure 4: Code snippet for the recursive algorithm of trapezoidal digital filter.

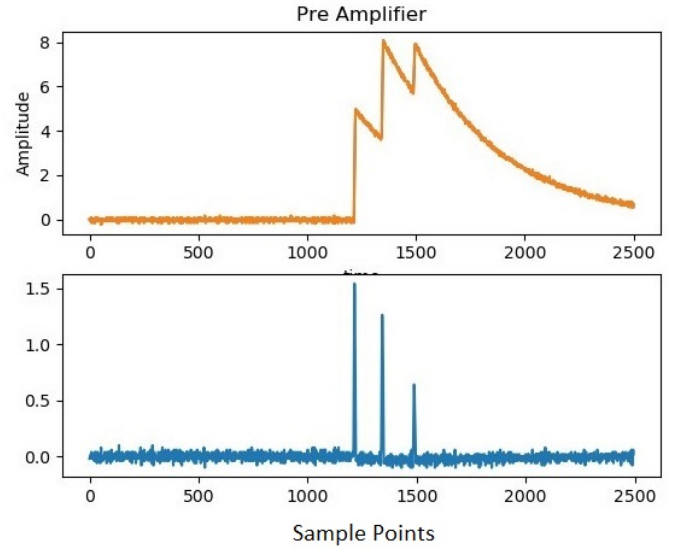


Figure 5: Output of trapezoidal filter with three input pulses.

3.2 Digital spectroscopy system

Pixels are applied to four separate preamplifier circuits, then four preamplifier outputs are combined using an output summed circuit. The output of the summed signal

of 4-channel and the individual pixels of arrays are applied separately to the 5-channel of CAEN digitizer, also collecting the output waveforms using the Cs-137 radioactive sources. The output of the digitizer is obtained as shown in Fig. 7 by the impact based SiPM detector. Each gamma radiation on a CsI(Tl) generated pulses of different heights according to the share of photons received from the source (Fig. 7). The summed output pulse, which has a higher rate than the output signal of each array is also shown in Fig. 8.

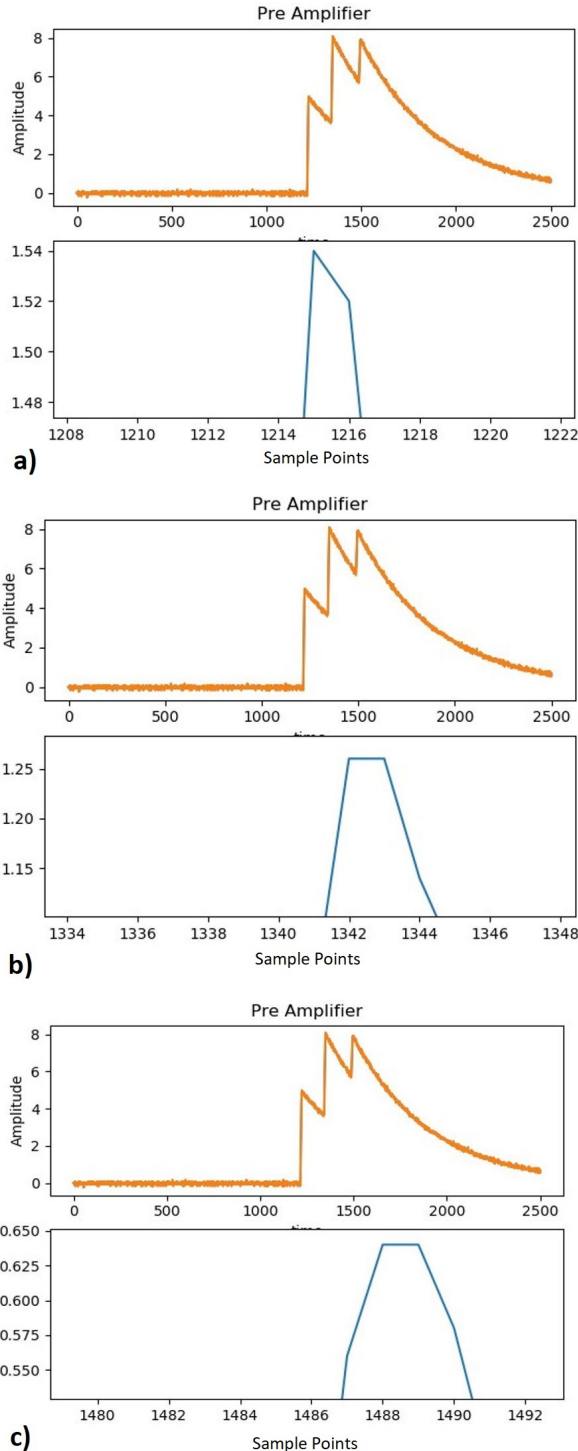


Figure 6: Zoom in on the output pulses of the trapezoidal filter based on the input pulses.

For digital spectroscopy, a prepared SiPM coupled CsI(Tl) detector and CAEN 8 channel digitizer were used. The specification of this digitizer board is in Table 1. As shown in Fig. 9 the output of each pixel of array and summed signal connected to 5-channel of the digitizer is seen.

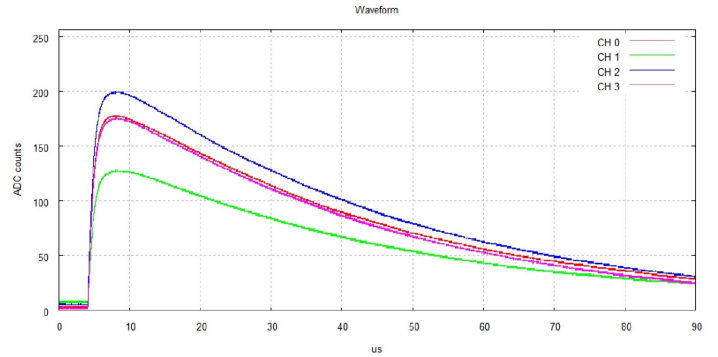


Figure 7: 4-channel output signal from the digitizer.

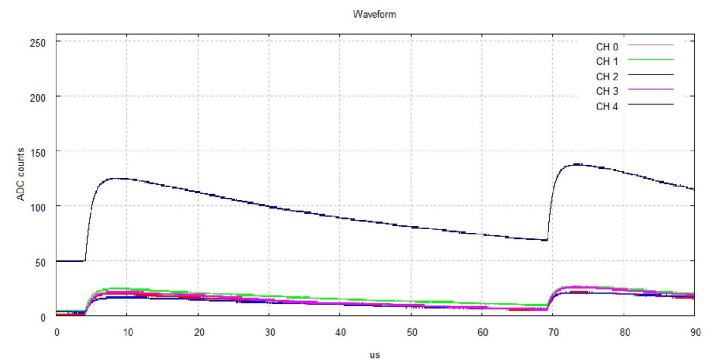


Figure 8: Digitizer output signal from each of the SiPM arrays 4-channel of SiPM array and summing of 4 channel show as Ch4.



Figure 9: Connecting the detector, preamplifier and collector assembly to the digitizer.

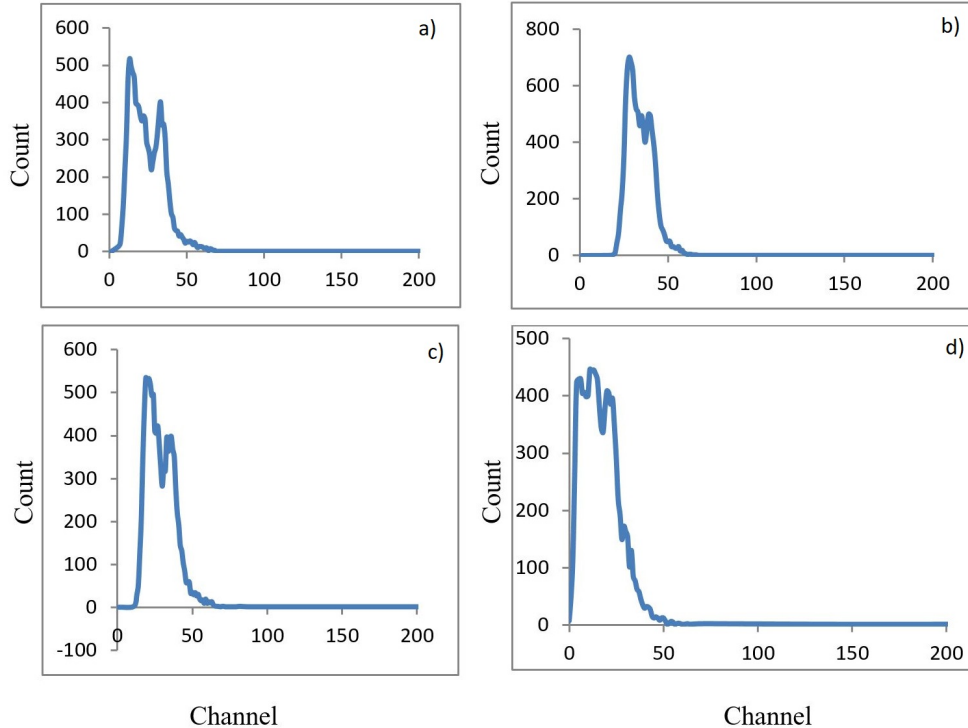


Figure 10: digital spectrum of each channel of SiPM, channel 1, 2, 3, and 4 spectrum are respectively shown in panels (a), (b), (c), and (d).

Table 1: CAEN digitizer specification.

Model	V1721 Standard VME
Input Channel number	8 channel
Sample Rate	500 MS.s ⁻¹
Input connector of channels	MCX
ADC Resolution	8 Bit

Table 2: Analog MCA Specification.

Model	FA-RD-MCA1
Channel Number	Selectable from 128 to 2045
Conversion Time	2 μ s
Maximum throughput	50000 CPS
Internal amplifier shaping	Fixed 1 μ s
ADC Successive approximation	12 bit

3.3 Digitally summed spectrum

The digital spectrum of each pixel was obtained in Fig. 10. Also, the summed spectrum of 4 arrays which was digitally obtained for Cs-137 is shown in Fig. 11. The resolution of this spectrum was calculated 9%, which is better than this channel resolution for the analog spectrum (Fig. 14).

3.4 Analog Spectroscopy system

The analog spectroscopy system and its specification are respectively presented in Fig. 12 and Table 2. Likewise, the calibration was done with two sources, Na-22 and Cs-137 and the calibration curve was obtained in Fig. 13.

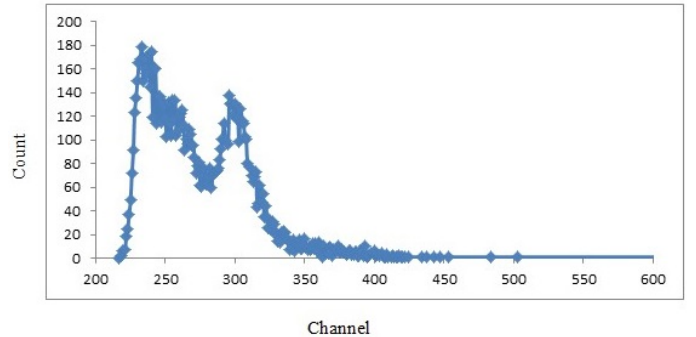


Figure 11: digitally summed spectrum of 4 channels of SiPM.

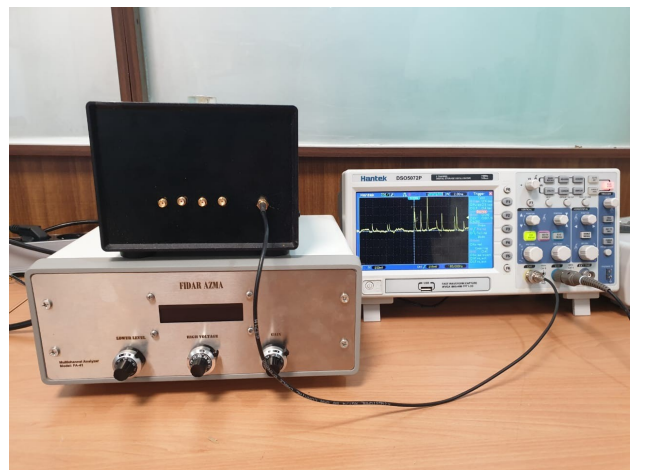


Figure 12: Connecting the detector, preamplifier and collector assembly to the digitizer.

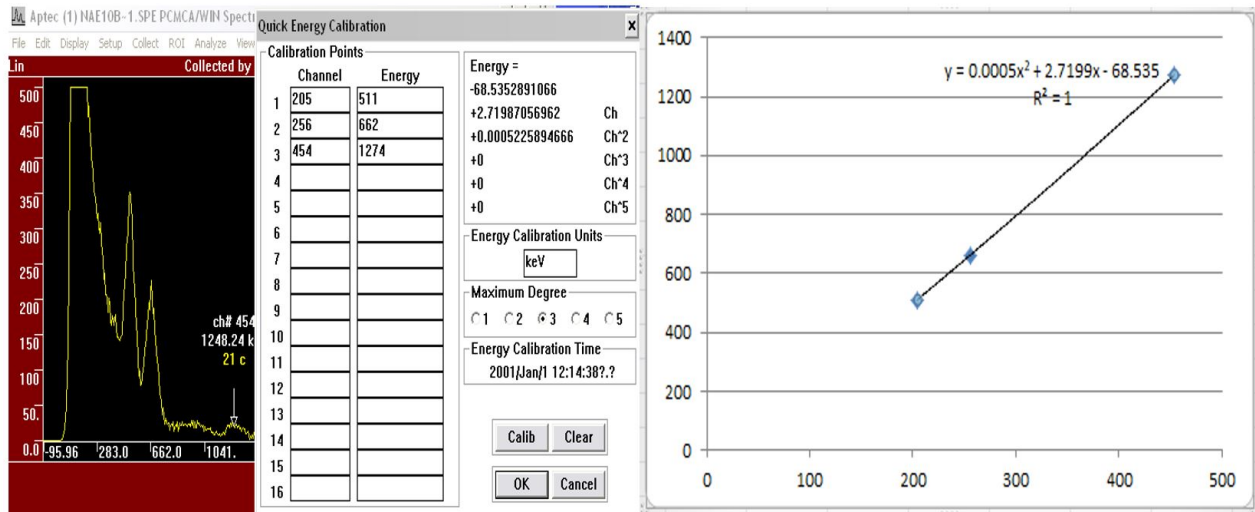


Figure 13: (a) Calibrating system with mixed source Cs-137 and Na-22, (b) Calibration Curve of spectrum.



Figure 14: Spectrum obtained from a 2×2 -pixel array detector when exposed to Cs-137 gamma ray source.

3.5 Detector calibration

Calculating FWHM needs energy calibration which has been done, as shown in Fig. 13. The calibration equations were obtained with three energy points related to Na-22 (511 keV, 1274 keV) and Cs-137 (662 keV).

3.6 Energy resolution

The energy spectra for SiPM coupled on CsI(Tl) with an energy window of 200 to 800 keV were obtained. Events were acquired using a Cs-137 source for 300 s in energy-spectrum mode. The pulse height spectra were measured

by ADC, via an output amplifier. Energy resolutions were calculated as FWHM by fitting the full-energy peaks with Gaussians, in percentage.

As mentioned in the introduction section, the goal of this study is to achieve the appropriate energy resolution. One of the steps taken to achieve this goal is to add the output of the arrays. In the digital method, the spectrum of each channel was summed; the FWHM calculated for this spectrum is 9%. By connecting the output of the amplifier pulses to the MCA (Multichannel Analyzer), the resulting spectrum of the 2×2 array detector based on the CsI(Tl) crystal can be seen in Fig. 14. FWHM (en-

ergy resolution) of 10.16% has been calculated through the offline data storage for this detector. The activity of gamma-ray source is $2.7 \mu\text{Ci}$.

4 Conclusions

In this research, the digital signal reading method has been used to receive and shape the output pulses of SiPM. Trapezoidal digital filters are used to properly shape the pulse. In this way, in the digital reading method, unlike the analog reading method, the output of the preamplifier is directly connected to the digitizer. The use of coupled SiPM/CsI(Tl) with integrated crystals on an array of SiPMs in turn destroys the resolution, and the use of analog methods will not have the desired result. In the digital method, the trapezoidal filter algorithm is implemented with the Python programming language in such a way that the output of each of the 4-channels shaped. Pixels are applied to four separate preamplifier circuits, then four preamplifier outputs are combined using an output summed circuit. The output of the summed signal of 4-channel and the individual pixels of arrays are applied separately to the 5-channel of CAEN digitizer and then the trapezoidal filter is applied to the output of the digitizer to shape a pulse. Also, digital spectrum of the 4-channel of SiPM were summed. The resolution of this digital spectrum was calculated 9%, which is comparable with analog spectrum. The resolution of the analog spectrum was calculated 10.16%. In the future, we will focus on optimizing weighting factor of each pixel.

Conflict of Interest

The authors declare no potential conflict of interest regarding the publication of this work.

References

- Aldawood, S., Thirolf, P., Miani, A., et al. (2017). Development of a Compton camera for prompt-gamma medical imaging. *Radiation Physics and Chemistry*, 140:190–197.
- Alispach, C., Borkowski, J., Cadoux, F. R., et al. (2020). Large scale characterization and calibration strategy of a SiPM-based camera for gamma-ray astronomy. *Journal of Instrumentation*, 15(11):P11010.
- Berti, A., Chiavassa, A., Corti, D., et al. (2020). Development and test of a SiPM cluster for a SiPM version of the Cherenkov Telescope Array LST camera. *Nuclear Instruments and Methods in Physics Research Section A: Accelerators, Spectrometers, Detectors and Associated Equipment*, 982:164373.
- Boo, J., Hammig, M. D., and Jeong, M. (2021). Row–Column Readout Method to Mitigate Radiographic-Image Blurring From Multipixel Events in a Coded-Aperture Imaging System. *IEEE Transactions on Nuclear Science*, 68(5):1175–1183.
- CAEN (2011). *CAEN Digital pulse height analyser- a digital approach to radiation spectroscopy, application note AN2508*. CAEN Digital pulse height analyser.
- Cates, J. W., Bieniosek, M. F., and Levin, C. S. (2017). Highly multiplexed signal readout for a time-of-flight positron emission tomography detector based on silicon photomultipliers. *Journal of Medical Imaging*, 4(1):011012.
- Cozzi, G., Busca, P., Carminati, M., et al. (2016). Development of a SiPM-based detection module for prompt gamma imaging in proton therapy. In *2016 IEEE Nuclear Science Symposium, Medical Imaging Conference and Room-Temperature Semiconductor Detector Workshop (NSS/MIC/RTSD)*, pages 1–5. IEEE.
- Czyz, S. A. and Farsoni, A. T. (2017). A radioxenon detection system using CdZnTe, an array of SiPMs, and a plastic scintillator. *Journal of Radioanalytical and Nuclear Chemistry*, 313(1):131–140.
- Frach, T., Prescher, G., Degenhardt, C., et al. (2009). The digital silicon photomultiplier principle of operation and intrinsic detector performance. In *2009 IEEE Nuclear Science Symposium Conference Record (NSS/MIC)*, pages 1959–1965. IEEE.
- Gnecchi, S., Barry, C., Bellis, S., et al. (2019). Long distance ranging performance of Gen3 LiDAR imaging system based on 1×16 SiPM array. In *Proceedings of the International Image Sensors Society (IIS) Workshop, Snowbird, UT, USA*, pages 23–27.
- Gnecchi, S. and Jackson, C. (2017). A 1×16 SiPM array for automotive 3D imaging LiDAR systems. In *Proceedings of the 2017 International Image Sensor Workshop (IISW), Hiroshima, Japan*, pages 133–136.
- Henningsen, F., Boehmer, M., Eller, P., et al. (2021). A self-monitoring precision calibration light source for the IceCube Upgrade. *Journal of Instrumentation*, 16(09):C09033.
- Huang, T., Fu, Q., Lin, S., et al. (2017). NaI (Tl) scintillator read out with SiPM array for gamma spectrometer. *Nuclear Instruments and Methods in Physics Research Section A: Accelerators, Spectrometers, Detectors and Associated Equipment*, 851:118–124.
- Jeong, M. and Hammig, M. (2020). Development of hand-held coded-aperture gamma ray imaging system based on GAGG (Ce) scintillator coupled with SiPM array. *Nuclear Engineering and Technology*, 52(11):2572–2580.
- Jiang, S., Lu, J., Meng, S., et al. (2021). A prototype of sipm-based scintillator compton camera with capacitive multiplexing readout. *Journal of Instrumentation*, 16(01):P01027.
- Kim, H., Kao, C.-M., Hua, Y., et al. (2021). Multiplexing readout for time-of-flight (TOF) PET detectors using striplines. *IEEE Transactions on Radiation and Plasma Medical Sciences*, 5(5):662–670.
- Kitsmiller, V. J. and OSullivan, T. D. (2019). Next-generation frequency domain diffuse optical imaging systems using silicon photomultipliers. *Optics Letters*, 44(3):562–565.
- Knoll, G. F. (2010). *Radiation detection and measurement*. John Wiley & Sons.
- Lavelle, C., Shanks, W., Chiang, C., et al. (2019). Approaches for single channel large area silicon photomultiplier array readout. *AIP Advances*, 9(3):035123.

- Lee, H., Lee, T., and Lee, W. (2020). Development of a position-sensitive 4π Compton camera based on a single segmented scintillator. *IEEE Transactions on Nuclear Science*, 67(12):2511–2522.
- Liang, Z., Hu, T., Li, X., et al. (2020). A cosmic ray imaging system based on plastic scintillator detector with SiPM readout. *Journal of Instrumentation*, 15(07):C07033.
- Maira, G., Chiarelli, A. M., Brafa, S., et al. (2020). Imaging System Based on Silicon Photomultipliers and Light Emitting Diodes for Functional Near-Infrared Spectroscopy. *Applied Sciences*, 10(3):1068.
- Press, W. H., Teukolsky, S. A., Vetterling, W. T., et al. (2007). *Numerical recipes 3rd edition: The art of scientific computing*. Cambridge university press.
- Shimazoe, K., Yoshino, M., Ohshima, Y., et al. (2020). Development of simultaneous PET and Compton imaging using GAGG-SiPM based pixel detectors. *Nuclear Instruments and Methods in Physics Research Section A: Accelerators, Spectrometers, Detectors and Associated Equipment*, 954:161499.
- Sun, Y. and Maricic, J. (2016). Sipms characterization and selection for the DUNE far detector photon detection system. *Journal of Instrumentation*, 11(01):C01078.
- Tétrault, M.-A., Lamy, E. D., Boisvert, A., et al. (2015). Real-time discrete SPAD array readout architecture for time of flight ET. *IEEE Transactions on Nuclear Science*, 62(3):1077–1082.
- Xiong, H., Zhou, R., Chen, J., et al. (2019). Design and performance of analog circuit for the wide field of view Cherenkov telescope array of LHAASO. *Nuclear Instruments and Methods in Physics Research Section A: Accelerators, Spectrometers, Detectors and Associated Equipment*, 925:156–163.
- Yang, Q., Kuang, Z., Sang, Z., et al. (2019). Performance comparison of two signal multiplexing readouts for SiPM-based pet detector. *Physics in Medicine & Biology*, 64(23):23NT02.

©2023 by the journal.

RPE is licensed under a [Creative Commons Attribution-NonCommercial 4.0 International License \(CC BY-NC 4.0\)](#).



OPEN ACCESS

To cite this article:

Berjisi, H., Pazirandeh, A. (2023). Spectroscopy of SiPM array detectors by digital spectroscopy method and implementing trapezoidal digital filter. *Radiation Physics and Engineering*, 4(3), 1-8.

DOI: [10.22034/rpe.2022.351237.1095](https://doi.org/10.22034/rpe.2022.351237.1095)

To link to this article: <https://doi.org/10.22034/rpe.2022.351237.1095>